Evaluation of the influence of carbide forming elements on microstructure and properties of ferritic ductile iron

The paper presents the results of a research project at the IfG in Düsseldorf during the last 2 years. The item of the activities was to investigate and evaluate the cumulative effects of carbide promoting elements on the microstructure and the properties of heavy-section castings made of ferritic cast iron like EN-GJS-400-15. The five selected carbide promoting elements manganese, chromium, niobium, vanadium and boron were varied in two levels. The result was an experimental design of $2^5 = 32$ trials. From each alloy were cast samples with different solidification conditions. On the specimen were evaluated the microstructure and mechanical properties. The generated data base with information about chemical composition, features of microstructure and also of the static, dynamic and cyclic mechanical properties and the fracture mechanics was analysed by multiple regression. As the main result of the project the paper presents regression equations for the formation of carbides and pearlite depending on the chemical composition on the one hand and for the influence of the structural constituents on the mechanical properties otherwise. During the project were used different software programs to calculate the carbide formation in complex cast iron alloys.

Gotthard Wolf, Wolfram Stets and Ulrich Petzschmann, Düsseldorf, Germany

Manuscript received 27 July 2011; accepted 7 November 2011

1 Description of the present situation

Spheroidal graphite cast iron (GJS) (defined by a European standard) has been used in many fields of mechanical engineering and vehicle building, as well as in the energy and environmental technology sectors. Scrap steel with percentages of up to 60 per cent is the most important material used in making it. For many years, steel making industries have developed steel of ever higher strength, used by the casting industries as new or recycled steel. This will inevitably also have repercussions on the casting industry and it comes with the additional disadvantage that so far nobody does have an understanding of the effects of the alloy elements, intentionally used to optimise material properties of resulting steels as far as microstructure and other properties of cast iron products are concerned.

Most of the alloying elements in the newly-developed steel varieties are carbide and perlite formers. Because of high carbon contents of the molten mass, these may form carbides already when present in small quantities. This means that heavy-section cast parts, in particular, with their long local solidification times, will be subject to the threat of segregation (concentrations of alloy elements in residual molten mass sections) in such parts. The relevance of this issue is on the increase as more and more heavy-section cast pieces are produced.

Foundries producing heavy castings are increasingly confronted with impairing scrap metal quality, because more and more elements like manganese, chromium, niobium, vanadium, and boron are being employed to make them. Even at low concentrations, these elements result in worsening ductility properties in ferritic cast iron types on account of the demanding combinations of such properties such as high ductility and sufficient strength. Such losses are the result of an increasing emergence of undesirable microstructural components, such as perlite and carbide. In heavy-section parts, in particular, and on account of segregation, large perlite areas in the presence of carbides emerge in the microstructure.

This paper offers a contribution that helps evaluate the cumulative influence of carbide forming elements like manganese, chromium, niobium, vanadium and boron on microstructure formation, thus dealing with properties as dependent on solidification conditions.

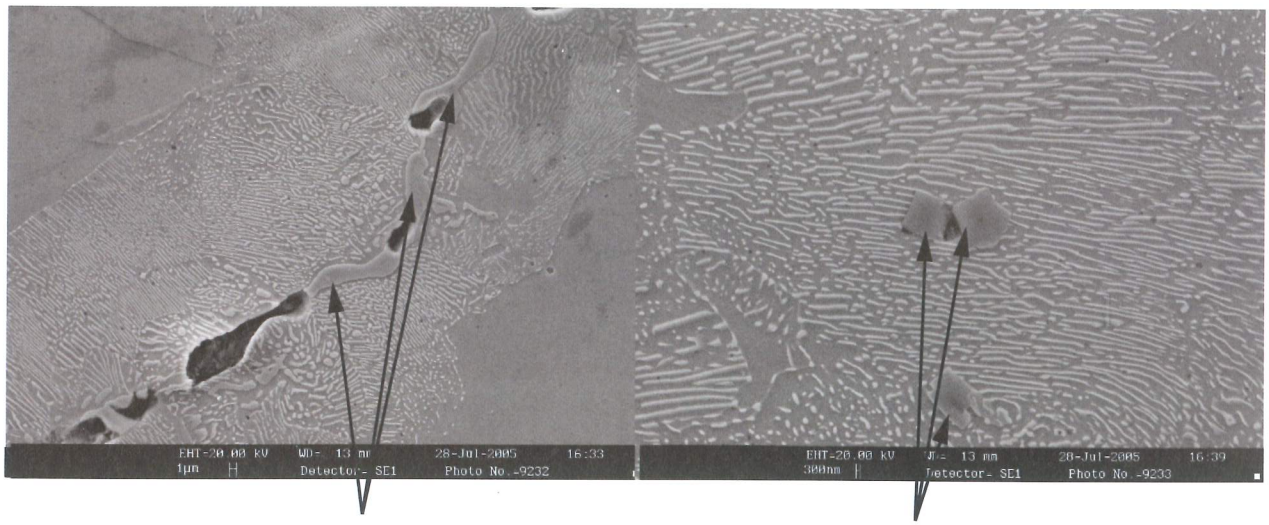

Figure 1: Segregations in heavy section castings grade GJS-400 lead to excessive formation of pearlite and carbides (chemical analysis/spectrometer: 0.02 % V; 0,035 % Cr; 0.015 % Ti)

2 What we know at present

Figure 1 shows carbide precipitation as seen in a heavy-section GJS-400 (defined by a European standard) cast part, being taken from a study of the Institute of Casting Technology (Institut für Gießereitechnik/IfG), Düsseldorf, Germany. This study proved that even small concentrations of alloy elements may result in carbide precipitation because of a combination effect.

The effects of individual trace elements on casting materials were debated in a number of studies [1-7]. W. Wolters und K. Roehrig [1] compiled a study on the effects of different elements on GJL microstructures, while K. Roehrig et al. did the same for GJS [2]. Also, Henke [3, 4] submitted a survey on the origins and the effects of alloy and trace elements. In this, combinations and interactions of elements with a carbide stabilising effect are assumed to be additive. Quite often, groups of elements may be set up for combinations of alloy elements, very frequently occurring together. Little is known about the joint effects of elements. Studies into this aspect are both very time-consuming and expensive.

J. F. Janowak and R. B. Gundlach [6] write on the influence of the most important alloy elements on the temperature situation in eutectic stable and meta-stable solidification (Figure 2) and they range them into different groups. Those (such as Cr, V, Ti), reducing the difference between eutectic temperatures, are carbide forming. Others, enlarging this difference, are stabilising the formation of graphite. This approach comes close to a description of these interrelationships in terms of thermodynamics, but only as far as qualitative properties are concerned.

R. Deike discusses basic considerations as to the importance and the effects of alloy and trace elements [7]. He deals with information offered in the literature and also describes the effects of these elements on eutectic solidification and eutectoid transformation.

T. Thielemann [8] introduces a "perlite value index" as helping to describe the effects of accompanying and trace elements for GJS. Employing two regression equations and the contents of such elements, the ferrite percentage may be cal-

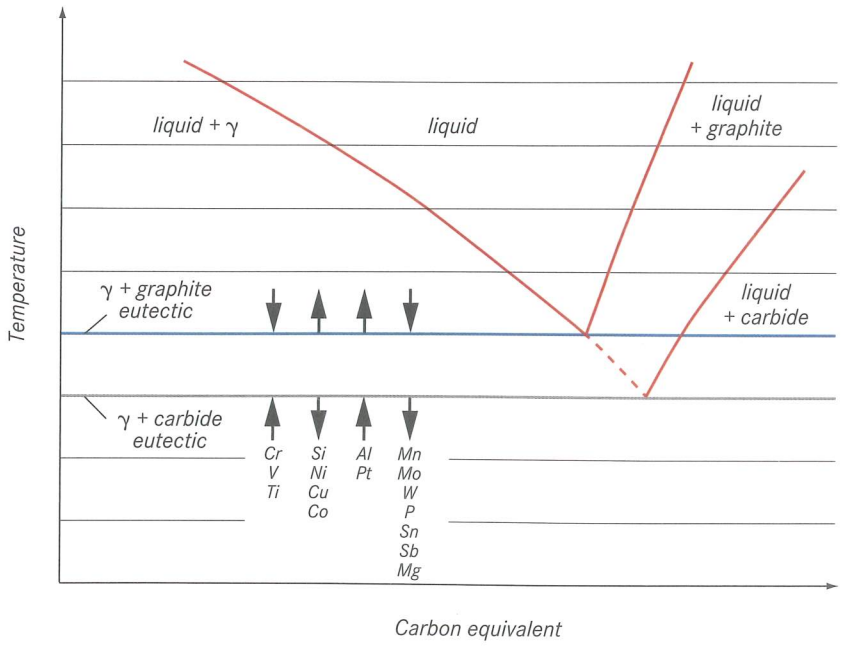

Figure 2: Influence of alloying elements on the stable and metastable eutectic temperature under equilibrium condition [6]

culated for two separately cast Y2-samples. Sample analysis was confined to the amounts of ferrite and perlite, the share of carbide in the microstructure was not a part of this study. No content limits were offered and elements like V, Nb, and B used in latest steel developments were not included.

An approach similar to that chosen by Thielemann was taken by W. Weis. He studied the influence of chemical elements on microstructure and chemical properties of ferritic cast iron with spheroidal graphite [9]. He developed a "perlite figure" employed by him to determine the perlite contents of separately cast Y2-samples. Additional regression equations were brought in to determine the relationships between mechanical properties, microstructure formation and chemical composition. He did not, however, submit any statements on the existence of carbides in microstructures. Because of the samples available (separately cast Y2-samples only) wall thickness dependence could not be analysed. This study again did not take into account latest alloy elements as used in steel development.

J. M. Motz [10] studied sprue samples (thickness 90 mm) of GJS-400 cast parts. He involved microanalyses to study concentration distributions of elements (Ti, Cr, S, Nb, and Zr). Though he found segregation of these elements, he was unable again to determine limiting values for them. The effects of segregation may be reduced if high numbers of spheres and a regular distribution of spherolites can be guaranteed. It is not possible, however, to guarantee large numbers of graphite balls for any range of wall thickness because of the influence the latter has on solidification times. As the number of spheres will be reduced with longer solidification intervals involved, segregation must always be considered when operating with greater wall thickness.

In a study devoted to the risks and limits for using micro-alloyed scrap steel C. Moex and W. Menk quote limiting values for V and Nb of 0.1 or 0.05 per cent, respectively, for cast iron with spheroidal graphite and with wall thickness ranging from 5 to 30 mm [11]. Additional studies [12-15] analysed the effects individual elements have on the microstructures and properties of cast iron. Henderieckx [16] divided carbide forming elements into eutectic or "chill" carbides and segregation conditioned, or "inverse chill" carbides. Like many other researchers, he uses his studies to determine limiting values for individual elements. Again and again, quality-related suggestions are offered concerning the cumulative effects of perlite- and carbide forming elements [11, 17].

Two papers looked into the cumulative interrelationships between perlite and carbide forming elements. For instance, Park and Gagne [18] studied the combined effects of manganese and chromium on microstructure formation in spheroidal graphite cast iron. Campomanes took one step further [19], when studying the cumulative effects of elements like silicon, manganese, chromium, vanadium and titanium on carbide formation.

Table 1: Levels of variables for the elements to be varied

Chemical elements	Level, %	
	Low level	High level
Mn	0.100	0.250
Cr	0.050	0.150
Nb	0.010	0.150
V	0.010	0.150
B	0.002	0.010

Studies available so far do not describe any interrelationship between wall thickness and the emergence of carbides and their effect on mechanical and fracture mechanical properties for heavy-section cast parts. As part of our research work carried out at the Duesseldorf Institute of Casting Technology, we studied the formation of perlite and carbides as well as the effects these have on static, dynamic and cyclic mechanical and fracture mechanical properties while considering elements like Mn, Cr, Nb, V, and B, increasingly found in scrap steel.

3 Experiments and studies

3.1 Planning and preparing for the experiments

The generation of a matrix for the main tests was based on the principle of experimental design. For each of the elements to be varied, both a high and low level (2 levels of variables) were determined. Determination of these levels was based on the results of literature studies, on experience available at the Duesseldorf Institute of Casting Technology as based on research projects and consultancy activities and also on assistance provided by representatives of

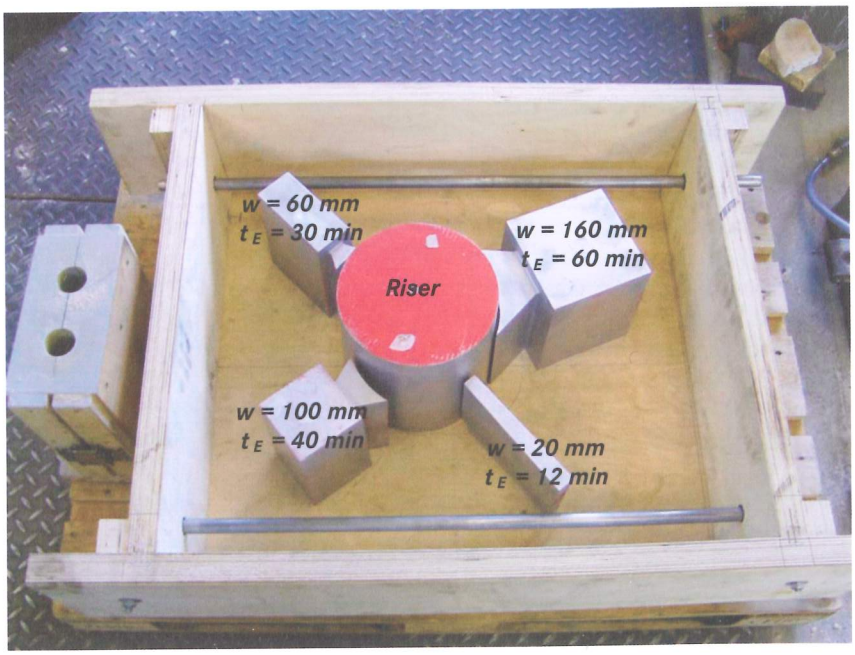

Figure 3: Pattern equipment for the propeller casting of matrix trials with different wall sections (w) and solidification times (t_E)

casting practice cooperating in a working group around this project. Assuming a linear behaviour of variables, the number of tests required was determined as follows:

$$n = 2^k = 2^5 = 32 \text{ tests} \quad (1)$$

n number of tests

2 number of levels of variables

k number of variables (elements)

The levels of variables for the elements to be varied were laid down as shown in Table 1.

The following were the limits for laying down the main elements:

- C: 3.45 % ±0.05 %,
- Si: 2.45 % ±0.05 %,
- Mg: 0.35 % ±0.05 %.

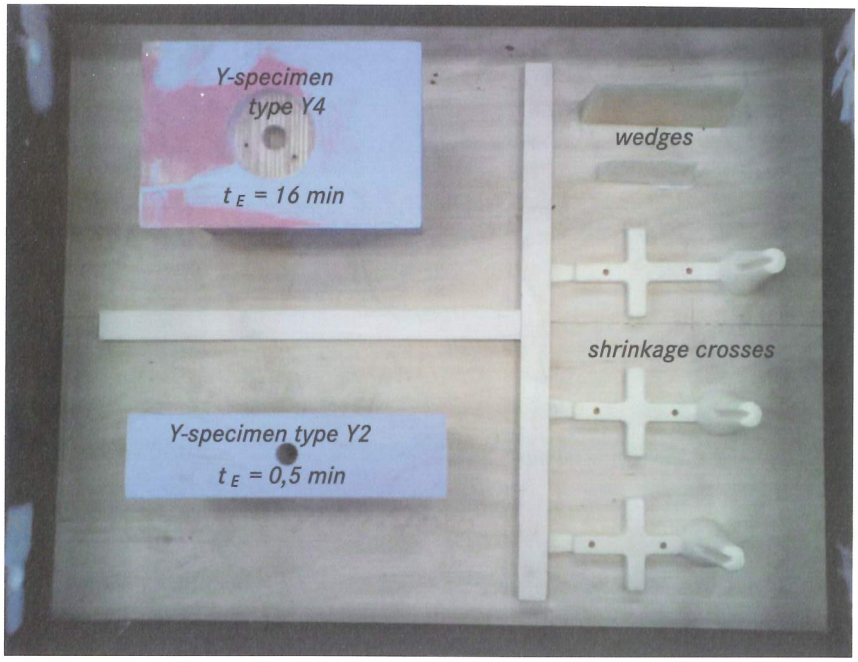

Figure 4: **Pattern plate for technological specimen**

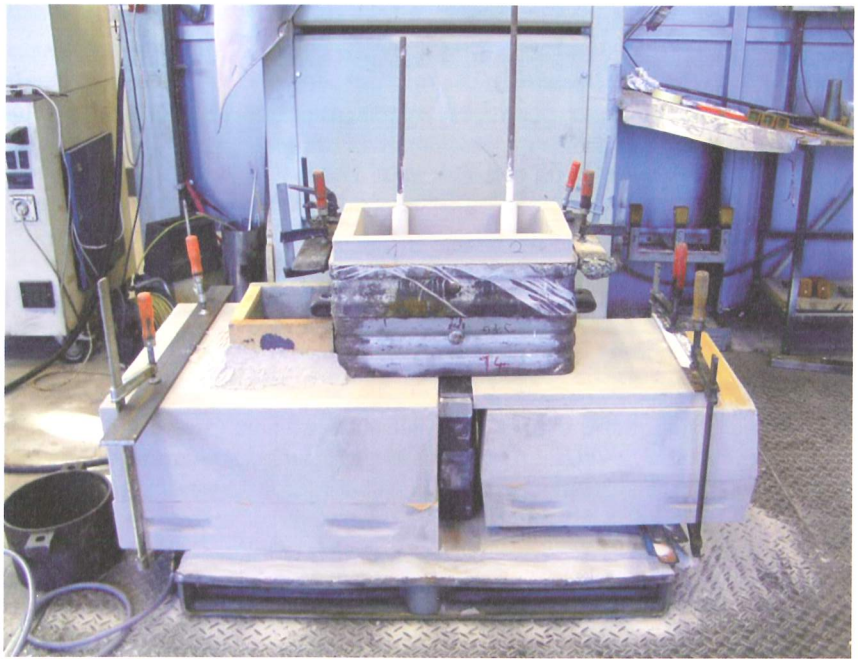

Figure 5: **Experimental setup with two moulds and a pouring basin with stoppers on the top**

Various aspects had to be referred to when determining test piece geometries. On the one hand, at the Duesseldorf Institute of Casting Technology facility the quantity of casting material is limited to 190 kg. On the other, the test piece must present different wall thicknesses in order to represent different cooling and solidification speeds. Also, technological samples had to be cast from the same casting operation (such as Y2 and Y4 samples). As a result of these demands, a "Flügelprobe" (propeller-like sample) was developed as a test piece (Figure 3) that presented different wall thickness dimensions (20, 60, 100, and 160 mm). The casting mould was gated in such a way as to enable a rising mould filling capacity. In addition to the "Flügelprobe", one mould was also cast with technological samples at the same time (Figure 4). The test set-up presented in Figure 5 was used for every casting operation to make sure that both moulds would contain molten mass of the same metallurgical quality after late-stage inoculation in the pouring basin. A number of preliminary tests were carried to work out an optimum test technology for all castings at the Duesseldorf Institute of Casting Technology. For a detailed presentation of all experimental and framework conditions please consult the final report [20].

3.2 Implementation and evaluation of tests

Samples were separated from the feeder and sawn in the middle of each casting. A microstructure sample was withdrawn from the very thermal centre of the test pieces. A metallographic evaluation of graphite and microstructure formation followed.

3.2.1 Metallographic analysis

The formation of graphite was studied and evaluated according to the DIN EN ISO 945 standard, employing the "dhs" automatic image analysing system. Assisted by this system, graphite formation was automatically determined and evaluated in five places.

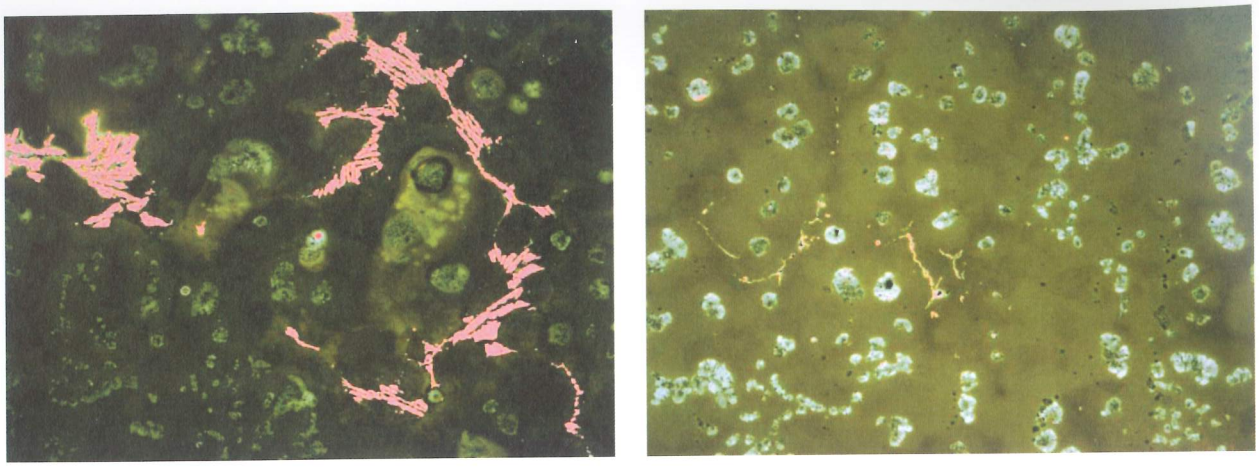

High level of carbides
Carbide fraction = 4.229 %

Low level of carbides
Carbide fraction = 0.194 %

Figure 6: Illustration of carbide evaluation based on the etching by Klemm type I

The ferrite/perlite ratio is the number one index to evaluate the matrix and this is determined as part of the automatic image analysis. The microstructure was further evaluated to find out about other microstructure components. Carbide formation was studied separately, as it was the most interesting feature.

To determine the carbide share in the microstructure, a semi-automatic procedure was developed as part of our project. For this procedure, a microsection will be etched following Klemm I, after graphite and matrix were evaluated, to achieve visibility of carbides in the microstructure (Figure 6). After this operation the microsection will be subjected to automatic image analysis. The system will detect whether there are surfaces taken up by carbides at five measurement points chosen at random and will then derive a mean value. As part of this analysis, a metallographic device will refer to evaluated image sections separately to eliminate those which might result in erroneous analysis because of etching errors or similar features.

As for their structure and composition, carbides were also analysed with a scanning electron microscope (SEM) and with the help of energy-dispersive X-ray spectroscopy (EDX) (Figure 7). Large-area carbide concentrations are always to be found in the perlite areas. Large areas of iron-chromium composite carbides are clearly visible, and also that they form distinguishable honey-comb structures. Vanadium carbides are to found in the vicinity of them, although they form separate entities. As a rule, these are thin and stretched out long – as basically already described by Dawson [13] before. As opposed to them, compact niobium carbides are distributed irregularly over the matrix. The emergence of these angular niobium carbides was similarly observed by Bedolla-Jacuinde et al. [12] and by Rivera et al. [15]. Their angular and compact structure leads one to assume that they are carbides primarily precipitated from the molten mass. Because of the fact that boron contents of a maximum of 0.01 per cent were below the EDX detection thresholds, boron could not be localised in the microstructure. In order to localise boron, an additional two experiments were carried out with boron concentrations of 0.03 per cent and 0.3 per cent, respectively. Cast iron with 0.3 per cent of boron had a carbide content of 19.8 per cent (Figure 8). This serves to underline the prominent position of boron when it comes to carbide formation. Regarding the way it tends to form carbides its influence is considerably larger than that of the other elements studied. Although the concentration of bo-

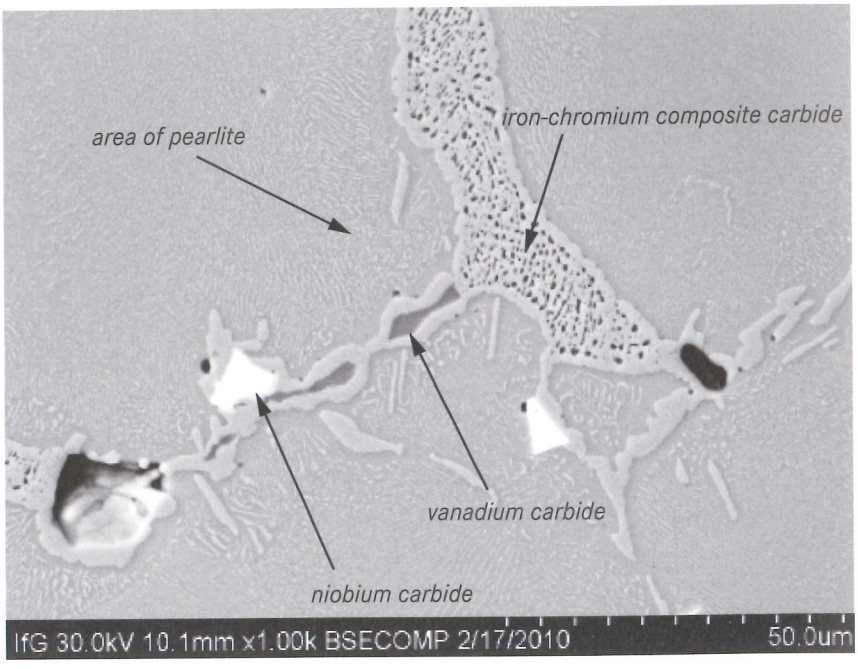

Figure 7: Typical carbides under the electron microscope

ron was significantly above the detection threshold, it was not possible to detect it in this microstructure with the help of EDX either. The reason for this is to be seen in the immediately contiguous positions of the intensity peaks for B and C, as a result of which B is superimposed by the high contents of C. Looking at the microstructure formation as we saw it, one may assume that boron as well as chromium will be deposited in the large-area iron-composite carbides (Fe_3C). Haofeng und Qunli have reported changes in the carbide structures resulting from the addition of boron [21]. They provide evidence to prove that the structure of chromium-containing carbides changes from honey-comb like to a herring-bone structure. This difference in carbide structure is obvious when comparing Figures 7 and 8. Independently of changes in the carbide structure it was observed that the carbide content goes up with the boron content and that graphite increasingly loses its spherical shape and a long-stretched degenerated form emerges.

3.2.2 Detection of statistical and dynamic mechanical properties

The determination of statistical and dynamic mechanical characteristic values was carried out in similar fashion as the metallographic studies at the Institute of Casting Technology. Samples for carrying out tensile tests, the notch-bar impact bending test and impact bending tests were collected from the opposing half of the micro section of cast parts. It was ascertained that samples were always picked from the same test piece segment. The following characteristic values were determined (always at room temperature):

- tensile strength Rm [N/m²] (following DIN EN ISO 6892);
- yield strength $Rp_{0.2}$ [N/m²] (following DIN EN ISO 6892);
- elongation A5 [%] (following DIN EN ISO 6892);
- reduction of area when breaking (following DIN EN ISO 6892);
- Young's modulus of elasticity (following DIN EN ISO 6892);
- notched-bar impact work (Charpy V notch test) (following DIN EN 10 145);
- impact work (10 × 10 × 55 not notched) (following DIN EN 10 045);
- Brinell hardness (HB) (following DIN EN ISO 6506-1).

In order to enable us to also study microstructure and property formation as dependent on wall thickness or local solidification time, respectively, local solidification time at the thermal centre of unalloyed master alloy test bodies was determined and used as the basis for ongoing studies.

3.2.3 Detection of cyclic and mechanical fracturing properties

Because of the considerable input required to study the series of properties, only four of each of the alloys were studied at room temperature. Material samples from test pieces used for these studies with a local solidification times of 60 minutes were purposefully chosen as for different microstructure features. Our objective was to find significant variations of carbide and perlite contents on the one hand and comparable graphite formation on the other.

The following were determined for materials samples of the four alloys:

- Compression-tension fatigue limit for R = -1 (following DIN 50 100 on samples according to ASTM E 466 und ISO 1099);
- Crack-resistance curves according to the J-integral concept (following ISO 12135).

Tests for compression-tension fatigue limits for R = -1 were carried out at the Institute of Casting Technology. Samples were tested on a high-frequency pulsator of the "Rumul Testronic 7001" type. Between 15 and 19 materials samples were tested of each alloy. For a statistical evaluation, SAFD 5.2 software of the Institute of material studies of Aachen University of Technology (RWTH), Aachen, Germany, was used. The results of an evaluation of these materials were summarised in stress-number curves for them.

Crack resistance behaviour parameters were studied at the Material Technology Institute of the Freiberg University of Mining and Technology, Freiberg, Germany. Static fracture toughness was determined following ISO 12135 using laterally-notched three-point bend samples (SE(B)-10 samples) at room temperature and a dimension to bottom of notch of 8 mm. A "Rumul Testronic 250"-type resonance testing machine was employed to generate fatigue cracks,

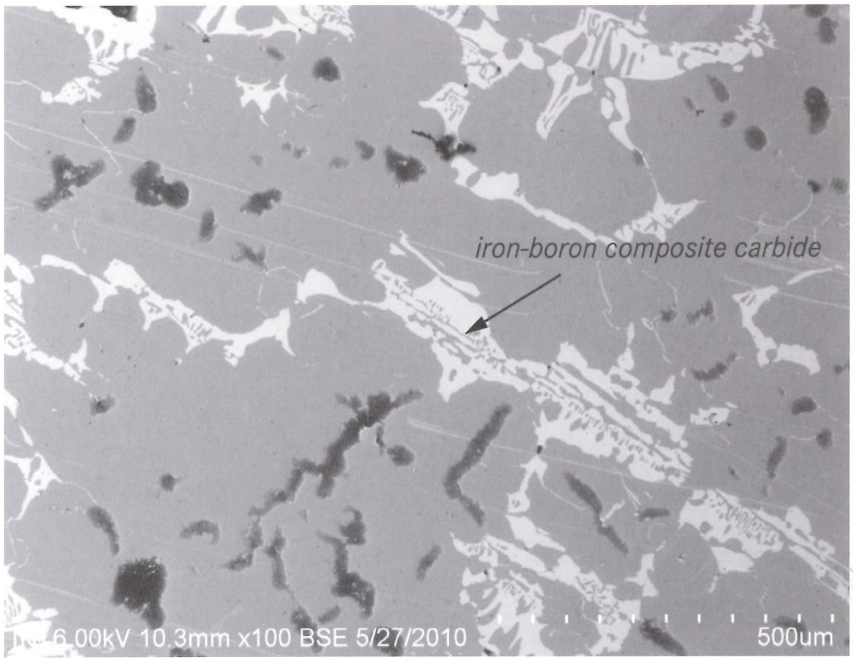

Figure 8: **Microstructure including 19.8 % carbides caused by a content of 0.3 % boron in the cast iron**

also at room temperature. Static tests were carried out after lateral notching. For this, a computer-controlled servo hydraulic testing device ("MTS 880") was employed.

Samples were then subjected to crack surface oxidation and broken up after intensive cooling to study crack areas. Stretch zones were measured with the help of a scanning electron microscope. In analogy to the determination of crack depth the determination of crack zone width must be carried out at nine locations. Following ISO 12135, any efforts to determine J_i, the physical crack initiation value, should eventually build on the crack resistance curve and by integrating critical stretch zone width, determined with the help of a scanning electron microscope. In the context of our studies of the crack resistance behaviour, however, it was not possible to derive a physical crack initiation value. The reason for this was an unequal formation of the area of stable crack extension, really quite typical of inhomogeneous materials. As a result, any measurements required of stretch zone extension in nine different locations as required under the ISO 12135 standard do not make sense. To make up for this and to characterise materials the technical crack initiation point $J_{0,2\,BL}$ was determined (following ISO 12135).

3.3 Test results

3.3.1 Studying microstructure-property relationships

3.3.1.1 Carbide and perlite formation

Test-derived data was subject to a comprehensive statistical analysis. The approach chosen was similar to that employed by Campomanes [19]. All regression ratios are detailed in our final report on this research project [20].

As the elements Mn, Cr, Nb, V, and B chosen for a statistical experimental plan are not only carbide but also perlite forming, regression analyses employed both carbide as well as perlite contents as target figures. Also, as silicon plays a major part as an essential ferritising and graphitising element in cast iron, it was included into these regression analyses. To study the influence on microstructure formation, regression analyses were therefore carried out for the following fundamental dependencies:

- Carbides = f (Si, Mn, Cr, Nb, V, B);

- Perlite = f (Si, Mn, Cr, Nb, V, B).

Considering the fact that carbide forming elements are also perlite formers and assuming also that there are interrelationships between different elements during carbide and perlite formation, another step was introduced to study first-order interrelationships as they influence the regression result. To do so, the products of all possible combinations of elements were included into these regressions. As it is possible in principle that individual elements do not have any linear influence on this regression, the second power of the elements selected was also integrated into this study.

All multiple regressions were based on the condition that the confidence interval of any term should at least be 95 percent. This guarantees that all terms are statistically relevant. On the basis of a higher significance for multiple interrelationships, an adjusted determination coefficient was employed in order to evaluate the quality of regression carried out.

For a local solidification time of sixty minutes, corresponding to a wall thickness of about 160 mm, the following regression ratios resulted for the carbide and perlite contents to be expected in the microstructure, depending on the chemical composition, of course:

$$\text{Carbide}_{60\,min} = 0.0155 + 2{,}241\,B^2 - 1{,}489\,B + 610\,B \cdot Si + 425\,B \cdot Cr + 964\,V \cdot B + 29.97\,Cr \cdot Nb + 18.54\,Cr \cdot V - 38.15\,Nb - V \quad (2)$$

adjusted $R^2 = 92.5\,\%$; $\sigma = 0.27$

$$\text{Perlite}_{60\,min} = 5.50 - 43{,}570\,B^2 - 17{,}386\,B + 149.1\,Cr^2 + 300.8\,Nb^2 + 1{,}824\,V - 34.90\,Si \cdot Nb - 722.4\,Si \cdot V + 7.447\,Si \cdot B + 564.6\,Cr \cdot Nb + 6{,}061\,Mn \cdot B - 7{,}472\,V \cdot B \quad (3)$$

adjusted $R^2 = 89.4\,\%$; $\sigma = 3.0$

A presentation of carbide contents as depending on wall thickness or on local solidification times measured for different wall strength dimensions on the one hand shows different carbide levels dependent on the contents of various carbide formers in the molten mass. It becomes obvious, on the other hand, that the alloy-dependent carbide content remains relatively constant up to a solidification time of 30-40 min (w = 60-100 mm) (**Figure 9**). As dependent on the chemical composition, a basic level of carbides is available in thinner walls. Only after solidification times continue growing, will there be an increasing separation of carbides. The sharp jump of carbide quantities in pieces with larger wall thickness leads one to assume that these are carbides separated in connection with segregation processes. Given increasing local solidification times, these segregation phenomena multiply in frequency.

An analysis of perlite contents reveals a fundamentally similar behaviour. However, as **Figure 10** and following regression analysis prove as well, perlite formation does not only depend on local solidification times but also on wall thickness. As regards thinner walls, cooling speed determines the degree of perlite formation next to chemical composition. Only as a result of increasing local solidification times will segregations occur in increasing numbers, given the presence of carbide and perlite. This then results in increasing perlite formation within segregation zones, as a result of which carbides will be precipitated within these regions.

Taking this fact into consideration, data was once again subject to multiple regression analyses, this time separated into two areas with different local solidification times. It became obvious then that up to local solidification times of forty minutes, carbide formation hardly depends on the latter. Given longer local solidification times, however, a significant increase in carbide contents becomes apparent and this regression ratio can be presented as follows:

$$\text{Carbide}_{40\text{-}60\,min} = -0.420 + 0.0108\,t_E - 2.043\,V + 3{,}910\,B^2 + 36.59\,Cr \cdot V - 20.28\,Nb \cdot V + 830.3\,V \cdot B \quad (4)$$

adjusted $R^2 = 87.6\,\%$; $\sigma = 0.31$

It remains an outstanding question and one still to be analysed in further studies whether this ratio shall also apply to local solidification times over and above sixty minutes.

The perlite content, however, is rising gradually across the whole range of different local solidification times ranging from 12 to 60 minutes. This interrelationship is also reflected in Figure 10. The link found that represents the dependence of perlite contents on the chemical composition and local solidification times can be described as follows:

$$\text{Perlite}_{12\text{-}60\,\text{min}} = 26.88 + 0.0999\,t_E - 485.3\,\text{Mn} + 33.23\,\text{Cr} + \\ + 1{,}033\,\text{V} - 4.86\,\text{Si}^2 + 92.66\,\text{Cr}^2 + \\ + 106.7\,\text{Nb}^2 + 199.8\,\text{Si}\cdot\text{Mn} - 407.4\,\text{Si}\cdot\text{V} + \\ + 5{,}178\,\text{Mn}\cdot\text{B} - 4{,}256\,\text{V}\cdot\text{B} \qquad (5)$$

adjusted $R^2 = 83.4\,\%$; $\sigma = 3.13$

3.3.1.2 The influence of microstructure formation on material properties

The microstructure of GJS* consists of graphite deposits and a metal matrix. Graphite should come in spheroidal dimensions, and as a result of lowering solidification times, there should also be a growing percentage of graphite forms IV or even III. The metal matrix is made up of ferrite and/or perlite. The ferrite/perlite ratio will adjust as it depends on the composition of the alloy, cooling conditions and the state of nucleation (graphite sphere numbers). Given the presence of perlite-forming elements, the quantity of perlite will be on the increase despite falling cooling speed. One of the reasons behind this is to be seen in the segregation of these elements, leading, in turn, to allied local changes in chemical composition. Also, and in the same manner, carbide forming elements lead to segregation, all the more that, as a rule, carbide formers are also perlite formers (such as Mn and Cr). This means that other components, such as carbides, may also exist in the microstructure. Given increasing wall thickness (reducing solidification), carbides will exist in association with perlite.

Ferritic GJS* comes with comparatively good ductility properties at satisfactory strength. These properties come about because of a high percentage of ferrite and sphere-shaped graphite. As a result of this, deviations in the form of graphite and increasing shares of perlite and carbides lead to reduced quality properties as far as toughness is concerned. The segregation of accompanying and trace elements goes up with increasing wall thickness; there will be increasingly large areas of perlite with growing carbide shares.

3.3.1.2.1 Static and dynamic mechanical parameters

Multiple regressions to describe the dependence of static and dynamic mechanical properties on graphite formation did not always bring up logical connections (such as the influence of type III graphite contents). However, to reach a position enabling us to evaluate the influence of the metal matrix (perlite and carbide share) on mechanical properties, regressions were limited to those alloys selected for determining cyclical and fracture mechanical parameters. As these samples come with a comparable graphite formation, these parameters were not included into the regressions. That means that the following links were established for a local solidification time of 60 minutes:

$$\text{Rm}_{60\,\text{min}} = 337.0 - 0.184\,\text{Perlite}^2 + 7.54\,\text{Perlite} \qquad (6)$$

adjusted $R^2 = 99.5\,\%$; $\sigma = 1.09$

$$\text{Rp}_{0.2\,60\,\text{min}} = 268.8 + 0.057\,\text{Perlite}^2 \qquad (7)$$

adjusted $R^2 = 96.4\,\%$; $\sigma = 3.65$

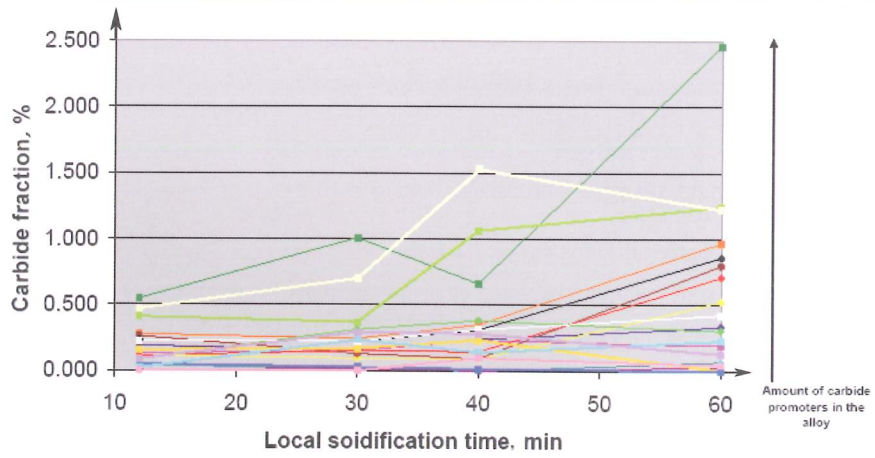

Figure 9: Carbide fraction depending on chemical composition and local solidification time (wall thickness)

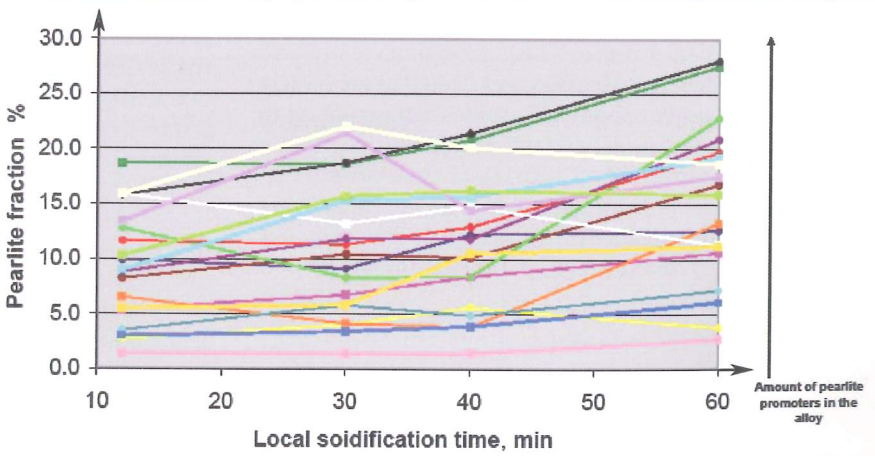

Figure 10: Pearlite fraction depending on chemical composition and local solidification time (wall thickness)

* *Translator's note: Terminology as laid down by DIN standards in Germany*

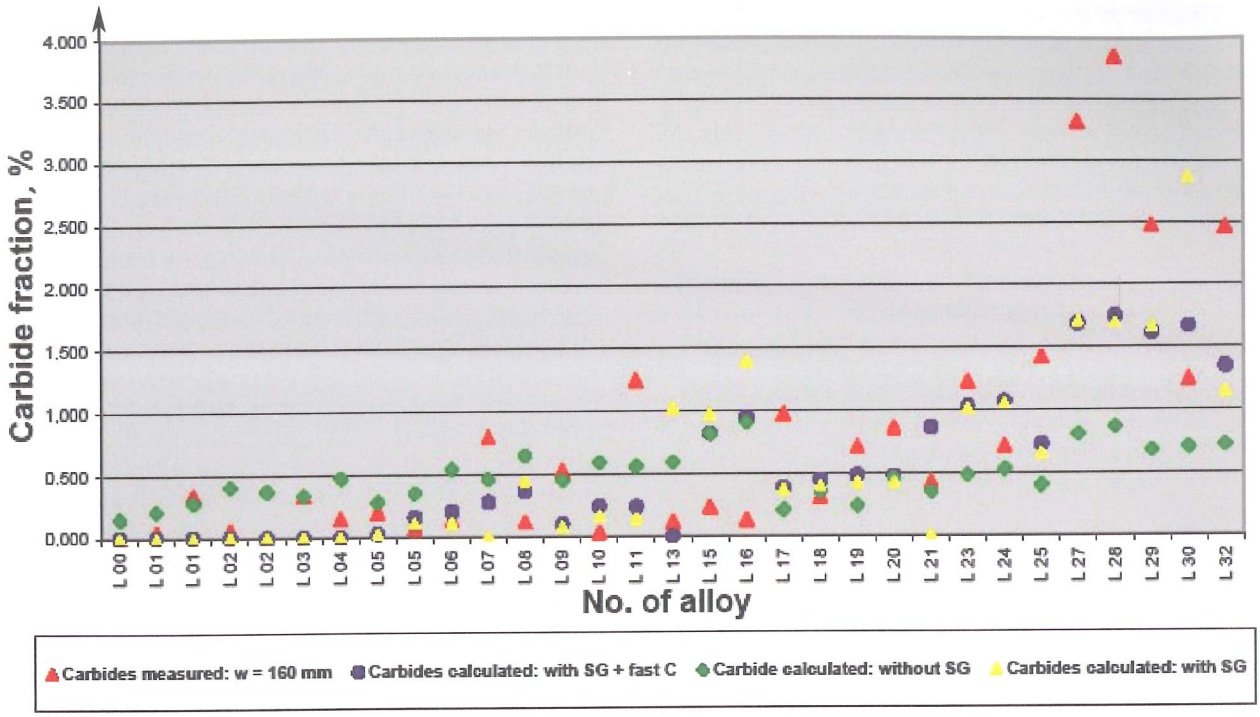

Figure 11: Comparison of experimental values of the carbide fraction at w = 160 mm with values calculated under the use of different methods

$$A5_{60\,min} = 18.83 - 0.6025\ Carbides^2 - 0.4075\ Perlite \quad (8)$$

adjusted $R^2 = 99.987\%$; $\sigma = 0.06$

$$IW_{60\,min} = 127.12 - 3.38\ (Carbides^2 + Perlite) \quad (9)$$

(Impact work)

adjusted $R^2 = 95.1\%$; $\sigma = 8.21$

$$\sigma_{CTFL\,60\,min} = 191.52 - 0.42\ e^{Carbides} \quad (10)$$

adjusted $R^2 = 95.1\%$; $\sigma = 2.42$

$$J_{0.2\,EaF\,60\,min} = 47.67 - 0.82\ Perlite \quad (11)$$

adjusted $R^2 = 99.94\%$; $\sigma = 0.20$

On account of the few and very closely-spaced characteristic values for notch bar impact work it was not possible to derive any statistically reliable relationship that did make sense. This equation will therefore not be included. One may assume, however, that there are dependencies which are similar to those of impact work (not notched specimen).

It is a striking feature that increasing mechanical strength properties (tensile strength and yield strength) are largely determined by perlite contents. Carbide contents of up to four per cent as were found in selected test materials, do not have any notable influence. Contrary to that, carbides result in a considerable reduction of ductility properties, already at comparatively low concentrations. The influence of perlite contents on both elongation and impact work is considerably smaller.

3.3.1.2.2 Cyclical and fracture mechanical characteristic values

Multiple regression analyses to determine dependencies of the compression-tension-fatigue limits and the technical crack initiation value of perlite and carbide contents at a local solidification time of 60 minutes brought out the following results:

3.4 Calculations to describe carbide formation

3.4.1 Calculations with the help of ThermoCalc®

Calculations involving ThermoCalc® were done using the TCFe6 data base. Different calculation models were employed in an attempt to pre-calculate carbide contents of the experimental alloys to be expected. Figure 11 summarises the results of different calculations when compared to experimentally-determined carbide shares of microstructures. It was only those calculations that were based on the Scheil-Gulliver approach and the definition of carbon as a rapidly-diffusing element that led to approximate results.

The problem is that the basic module of the software employed may only be used for calculating states of equilibrium. Although the Scheil-Gulliver model considers diffusion in the liquid stage and thus offers at least an approach to segregation, this model will only work reliably up to 99 per cent of solidification. That is to say, during the final one per cent of solidification and only when the larger percentage of carbides will be precipitated, the model ceases to offer any reliable results.

This model may therefore only be employed for approximate calculations when trying to predict carbide shares in microstructure.

The formation of carbides follows generally recognised mechanisms as shown in Figure 12 and they were described in [22], amongst others. Carbide forming elements raise the eutectic temperature of the metastable solidification (Figure 3). That means that this temperature shall be undercut during undercooling (at an impaired state of nucleation) and towards the end of the solidification process. Depending on when this metastable eutectic temperature will be undercut, different carbides will be precipitated. Henderickx [16] differentiates between eutectic carbides and segregation carbides in such a situation. Eutectic carbides will be precipitated when too much undercooling of the molten mass occurs. This may be the result of excessive cooling speed or because of a bad state of nucleation. During long periods of solidification segregation carbides will only be precipitated at the end of this solidification process and when a metastable eutectic temperature will be undercut before solidus temperature was reached (Figure 12). Based on this theory the following relevant temperatures were calculated for the experimental alloys:

- the eutectic temperature of metastable solidification, and
- the solidus temperature (= the "end of solidification" shown in Figure 12).

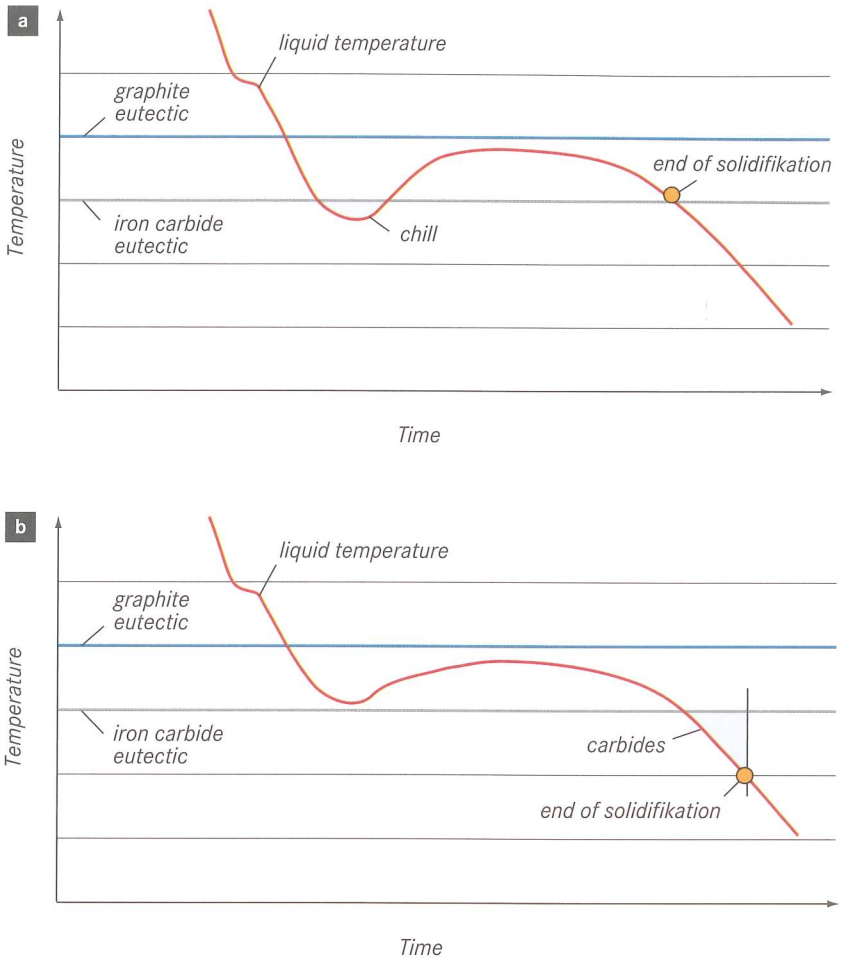

Figure 12: Mechanisms for the formation of carbides: b) formation of segregation carbides caused by the underrun of the metastable eutectic temperature before the end of solidification [22]

This calculation used ThermoCalc® (Scheil-Gulliver model; rapidly diffusing C). The carbon contents measured were entered as a function of the temperature difference of the temperatures listed above (Figure 13). It becomes obvious that the share of carbides in the microstructure of a wall with a local solidification time of sixty minutes goes up with the difference between the solidus temperature and the metastable eutectic temperature. There is a good correlation between the carbide contents measured and the temperature differences calculated. The resulting ratio for a local solidification time of sixty minutes is as follows (Figure 13):

$$\text{Carbide}_{60\,\text{min}} = 0.0009\,\Delta T^3 - 0.0117\,\Delta T^2 + 0.1151\,\Delta T \quad (12)$$

$$(R^2 = 86.4\,\%)$$

$$(\Delta T = T_{\text{eutectic/metastable}} - T_{\text{solidus}})$$

3.4.2 Calculation with the help of Micress®

Unlike ThermoCalc® Micress® can consider kinetic effects during solidification. Model calculations were carried out for three selected alloys, using the same data base. Doing so, it was possible for the first time to simulate a spatially-resolved solidification of a cast iron alloy, even though a number of calculation-technological approximations had to be used because of the degree of complexity of the alloys dealt with. A satisfactory agreement between carbide shares calculated with those determined in experiments was reached for two of the alloys chosen. In case no. 3 there is a significant deviation of one decimal power factor (Figure 14).

4 Summary

4.1 Results

4.2.1 Microstructure formation

- Up to a local solidification times of about 30 to 40 minutes, the carbide contents as dependent on the share of carbide forming elements are relatively constant. Practically speaking, there is hardly any dependence on wall thickness.
- It is only after a local solidification time of over 40 minutes that more and more segregation carbides will be precipitated.
- As carbide forming elements are also perlite formers, carbide formation in heavy-section cast parts must at all times be analysed in the context of perlite formation.

- Contrary to the carbide share in the microstructure, the perlite share already rises also in case of shorter local solidification times.
- Regression ratios were found to describe the dependence of perlite and carbide shares in the microstructure on local solidification times.

4.2.2 Properties

- Static mechanical characteristic values are mainly dependent on the perlite content (increases of Rm and $Rp_{0.2}$ given a higher perlite share in the microstructure).
- Ductility properties are preponderantly dependent on carbide content (decreasing A5 and impact work, or AV with an increasing carbide share in the microstructure).
- The compression-tension fatigue limit (R = -1) is primarily brought down by carbides in the microstructure.
- The technical crack-initiation value, however, falls off with increasing perlite content.
- For the dependency relations of static, dynamic and cyclic mechanical properties as well as for fracture mechanic indices it was possible to set up regression ratios for a dependency of these properties on the shares of perlite and carbides in the microstructure.

4.2.3 Calculations

- Only under very specific conditions may ThermoCalc® software be used for calculating carbide formation in complex cast iron alloys.

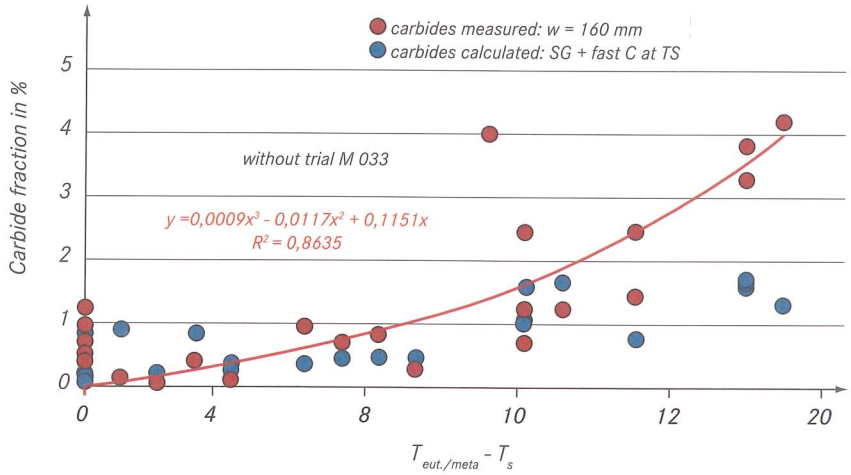

Figure 13: Comparison of experimental data with values calculated using Thermo-calc® for the carbide fraction depending on the temperature difference between the metastable eutectic temperature and the solidus temperature taking into account the chemical composition

Calculations with MICRESS®

(ACCESS e.V. Aachen)

- *consideration of kinetic influences*
- *based on the mulitphasearea-concept*
- *assumption of nodule count*

Trial	Mn [%]	Cr [%]	Nb [%]	V [%]	B [%]
M 005	*0.11*	*0.053*	*0.048*	*0.018*	*0.002*
M 013	*0.097*	*0.16*	*0.0103*	*0.15*	*0.0017*
M 02	*0.11*	*0.056*	*0.13*	*0.15*	*0.0019*

Calculated distribution of elements after solidification

	M005	M005 (exp)	M013	M013 (exp)	M020	M020 (exp)
cementite (at%)	0,333	-	1,74	-	1,29	-
cementite (vol%)	0,261	-	1,36	-	1,01	-
NbC (at%	0,0496	-	0,0079	-	0,075	-
NbC (vol%)	0,0892	-	0,014	-	0,135	-
VC(at%)	0	-	0,0495	-	0,132	-
VC(vol%)	0		0,0717	-	0,191	-
Nodule count l/mm²	208	141	208	142	260	176
Summary of carbides (vol%)	**0,350**	**0,194**	**1,45**	**1,248**	**1,34**	**0,113**

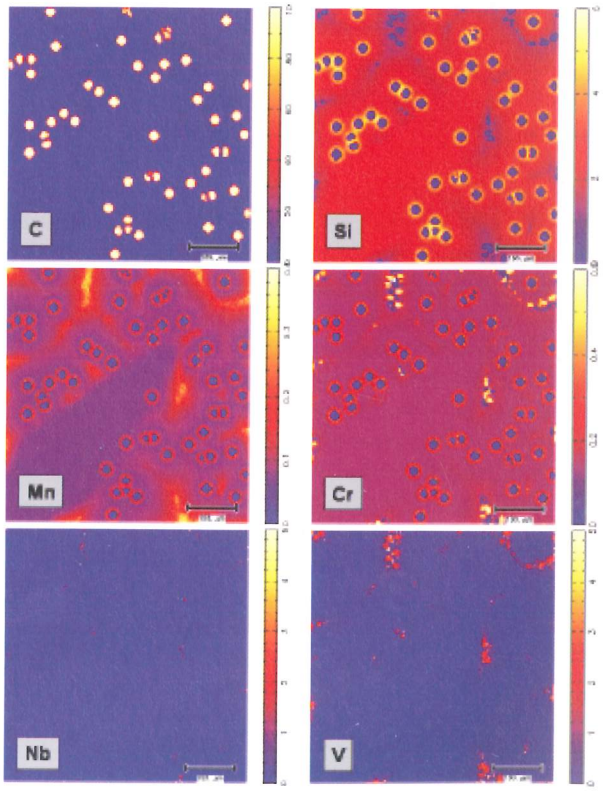

Figure 14: Results of the calculations of solidification and carbide formation with Micress®; images on the right: calculated distribution of different elements for alloy M 013

- For the first time, and using Micress® software, it has become possible to simulate solidification of complex cast iron alloys, even though some assumptions and simplifications had to be resorted to. It was possible in two of three cases to achieve good agreement with experimental results.
- The temperature difference between the alloy-dependent eutectic temperature of a metastable solidification and the solidus temperature is well correlated with the carbide shares in the microstructure as determined by experiments.

4.3 Prospects

Within certain limits and relying on the regression ratios defined it becomes possible to predict perlite and carbide formation in the microstructure and to evaluate the property changes to be expected on their account. Additional studies shall be required to find out whether this ratio will also apply to local solidification times of more than 60 minutes.

A number of inter-relationships between certain elements are described in the literature (such as [18, 19]). Bearing in mind the well-known cross-diffusion effects of silicon with directly segregating elements, such as Mn and Cr, one may assume that the interrelationships found for silicon with the carbide and perlite formers analysed in this study do really exist. It remains an interesting objective of further studies to examine the effects of additional elements inclusive of their own interactions. Campomanes [19] for instance, found significant interactions in the presence of Ti, but without giving consideration to the influences of Nb and B. This study, however, did not consider Ti as it was confined to the variation of carbide forming elements as Mn, Cr, Nb, V, and B. Molybdenum, however, remains another element to be studied.

The first-ever Micress® calculations for cast iron alloys revealed promising approaches. The methodology worked out needs to be confirmed by on-going calculations.

The interrelationship found between carbide formation and the temperature difference between the eutectic temperature and metastable solidification and the solidus temperature is quite interesting and needs to be further substantiated. Examinations shall have to be carried out on whether this method may be used to evaluate the tendency of molten mass for carbide formation even before casting, relying for this purpose on data gathered from traditional thermal analysis.

This IGF project, no. 15803 N, of the Research association of casting technology, a registered association, (FVG), located at Sohnstrasse 70, 40237 Düsseldorf (Germany), was supported via the Working group for industrial research communities (AiF) in the context of the Programme to promote industrial community research (IGF) by the Federal Ministry of Economics and Research of Germany on the basis of a decision by the German Bundestag. We would like to express our warm gratitude for this.

We would also like to thank the casting companies, contributing to the success of this research project of the working group involved. Special thanks go out to the "Metallwerk Franz Kleinken GmbH", which provided the opportunity to run operational tests in the context of this project.

***G. Wolf, W. Stets** and **U. Petzschmann,** Institute of Casting Technology (Institut für Gießereitechnik/IfG), Sohnstraße 70, 40237 Düsseldorf, Germany*

Literature:

[1] Wolters, W.; Röhrig, K.: Legiertes Gusseisen. Band 1. Gießereiverlag, Düsseldorf, 1970.
[2] Röhrig, K.; Gerlach, H.-G.; Nickel, O.: Legiertes Gusseisen. Vol. 2. Gießereiverlag, Düsseldorf, 1974.
[3] Henke, F.: Giesserei-Praxis (1971) no. 8, pp. 139-149.
[4] Henke, F.: Giesserei-Praxis (1971) no. 9, pp. 157-169.
[5] Neumann, F.; Schenk, H.; Patterson, W.: Giesserei 47 (1960) no. 2., pp. 25-32.
[6] Janovac, J. F.; Gundlach, R. B.: Giesserei-Praxis (1983) no. 15/1, pp. 223-242.
[7] Deike, R.: Giesserei 86 (1999) no. 6, pp. 175-182.
[8] Thielemann, T.: Gießereitechnik 16 (1970) no. 1, pp. 16-24.
[9] Weis, W.: Giesserei-Forschung 35 (1983) no. 1, pp. 1-13.
[10] Motz, J. M.: Giesserei 75 (1988) no.18, pp. 534-540.
[11] Möx, C; Menk, W.: Giesserei-Praxis (1994) no. 11/12, pp. 301-307.
[12] Bedolla-Jacuinde, A.; Solis, E.; Hernandez, B.: Effect of niobium in medium alloyed ductile cast irons. Int. Journal of Cast Metals Research 16 (2003) no. 5, pp. 481-486.
[13] Dawson, J. V.: Vanadium in cast iron. Paper of the 49th International Foundry Congress, 14-17 Aril 1982, Chicago, USA.
[14] Bauer, W.: Die Auswirkung kleiner Borgehalte auf die Ferrit-/Perlitbildung im Gusseisen. Giesserei 96 (2009) no. 4, pp. 22-31.
[15] I. Rivera, L.; Roca, A.; Patino Cardona, F.; Cruells, M.: Microalloyed niobium influence on ductile ferrite cast irons. Int. Journal of Cast Metals Research 16 (2003) no. 1-3, pp. 65-70.
[16] Henderieckx, S.: Carbides in ductile iron. Foundry (2007) Jan./Feb., pp. 29-32.
[17] Leaflet "Deutsches Roheisen" no. 1.459. 3. revised edition, 1984.
[18] Park, Y. J.; Gangne, M.: Die kombinierte Wirkung von Mangan und Chrom auf das Gefüge von Gussstücken aus Gusseisen mit Kugelgraphit. Giesserei-Praxis (1986) no. 15/16, pp. 209-216. AFS Transactions 91 (1984), pp. 387-393.
[19] Campomanes, E.; Goller, R.: The effect of certain carbide promoting elements on the microstructure of ductile iron. AFS Transactions 87 (1979) paper no. 79-174, pp. 619-626.
[20] Petzschmann, U.: Entwicklung einer Kennzahl zur Bewertung der kumulativen Wirkung von Karbid bildenden Elementen auf die Eigenschaften von GJS-400-15. Final report on AiF project no. 15803N, IfG-Institut für Gießereitechnik, Düsseldorf, Germany, 2011.
[21] Haofeng, Z.; Qunli, R.: Effects of boron and chromium on the morphology and wear-resistant properties of low-manganese cast iron. Indian Foundry Journal (1987) October, pp. 17-21.
[22] Gundlach, R. B.; Janowak, J. F.; Bechet, S.; Röhrig, K.: On the problems with carbide formation in gray cast iron. Mat. Res. Soc. Symp., Proc. vol. 34, 1985. Pp. 251-261.

Keywords: Ferritic ductile iron, pearlite, carbide, chemical composition, mechanical properties, multiple regression